International Journal of Power Electronics and Drive Systems (IJPEDS)
Vol. 15, No. 2, June 2024, pp. 685~695
ISSN: 2088-8694, DOI: 10.11591/ijpeds.v15.i2.pp685-695

Comparative study of passive magnetic bearing using four ring magnets: a critical review

Yang Chaojun[1], Amberbir Wondimu[1], Ayodeji Olalekan Salau[2,3]
[1]School of Mechanical Engineering, Jiangsu University, Zhenjiang, China
[2]Department of Electrical/Electronics and Computer Engineering, Afe Babalola University, Ado-Ekiti, Nigeria
[3]Saveetha School of Engineering, Saveetha Institute of Medical and Technical Sciences, Chennai, India

Article Info

Article history:

Received Jul 31, 2023
Revised Nov 17, 2023
Accepted Dec 7, 2023

Keywords:

Frictional losses
Load bearing
Magnet ring
Magnetic bearing
Small scale wind turbine
Stiffness

ABSTRACT

This is crucial because a significant amount of energy is wasted due to friction in the main roller bearing. In order to overcome this, the concept of levitation has gained popularity. Levitation is achieved by employing the repelling forces between two opposing poles of a permanent magnet (PM), significantly reducing friction between the turbine stator and rotor. As a result, the overall energy production of the turbine increases. The use of passive permanent magnet bearings has several disadvantages, such as limited load-bearing capacity and rigidity. To address these limitations, we conducted numerical studies on four different configurations in order to enhance load-bearing capacity and stiffness. The results showed that the radial configuration outperformed the axial-type configuration in terms of stiffness and load-bearing capabilities in all four arrangements. Furthermore, it was revealed that radial passive magnetic bearings with adequate air gaps are not only more efficient but also less expensive than employing iron cores at the rear and between ring magnets for small-scale wind turbines.

Corresponding Author:

Amberbir Wondimu
School of Mechanical Engineering, Jiangsu University
Zhenjiang, Jiangsu, China
Email: ambirewondimu@gmail.com

1. INTRODUCTION

Friction that arises when the various parts of mechanical components move against each other leads to substantial energy waste within the system, especially in wind turbine systems. Ball bearings have been employed to minimize these losses caused by friction. Minimizing these losses is crucial to maximizing the net output of the small-scale wind turbine. Advancements in magnetic materials have increased the utilization of magnetic bearings in various mechanical systems, effectively avoiding most frictional losses [1]–[7].

There are various types of magnetic bearings (MBs) that offer a noncontact mechanism of operation [8]–[15]. Thus, MBs have a long life, are free of lubrication, are quiet, have low stiffness, and thus vibration doesn't pass to the main machine housing. Passive magnetic bearings (PMBs) have recently gained significant attention from researchers and engineers due to their uncomplicated design and cost-effectiveness. Earnshaw's theorem states that it is impossible to construct a completely isolated magnetic suspension system. As a result, for magnet-suspended rotors, the controller needs to remain active while the other components can function passively [16]–[24]. Different types of passive magnetic bearings are available, such as superconducting, hybrid, and permanent magnet (PM) varieties. The PM category can be further divided into three specific topologies: axial, radial, and conic [22]–[26].

Stiffness plays a significant role in choosing PMBs for specific purposes. As discussed in the cited references [27]–[30], the magnetic charging technique has been demonstrated as a useful approach for determining the stiffness of axial or radial magnetic bearings in three-dimensional (3D) space. Nonetheless, in cases where the air-gap length of the magnetic bearing is shorter than the average air-gap radius, employing two-dimensional (2D) analytical and finite element methods for analysis proves to be more effective and efficient. These methods offer advantages such as reduced time, cost, and space requirements, as indicated in [31]–[38]. This study considers the magneto-static type of stiffness due to only the magnetic force effect [39]–[46]. PMB configurations such as axial [16], [47]–[52] and radial [53]–[55], with an iron core at the back [56]–[59], in between, and an air gap [60]–[63] in between four ring magnets are addressed. Stiffer PMB is recommended for small wind turbines for effective use of low-rated wind energy residential power consumption. The main goal of this critical review is to identify the stiffer PMB among four different arrangements and select the one most suitable for a small-scale wind turbine.

2. DESIGN CONFIGURATION

The design establishes a specific layout for a 2D electromagnetic model of PMBs. Figure 1 illustrates the technical root of the simulation. Each step and its corresponding execution in COMSOL multi-physics 5.6 will be examined. The geometry is established, and the selection of bearing materials is made, with the electromagnetic model's physics defined based on the model's specific objectives. The subsequent steps in finite element analysis (FEA) involve the creation of a mesh, which could be considered a form of artistic expression. Once the simulation jobs are completed, the results become accessible. Data is extracted from data sets and portrayed through 2D plots, providing a visual representation of magnetic flux density.

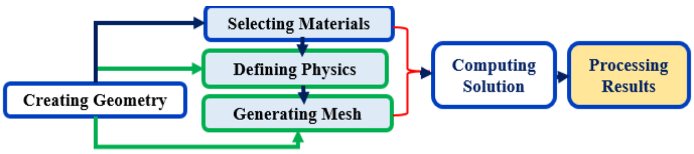

Figure 1. General workflow of a numerical analysis by finite element (FE) tool

The common structure of PMBs consists of two or three magnets in the stator and rotor, which are configured in front of each other. Assumptions were made while computing force and stiffness [45], [64]–[68], but in this study, we used four ring magnets to increase the rigidity of the structure, which makes it stiffer than ever:

- Air gap length (h) is smaller than the mean radius of air gap (r_h), 2D model is best to compute the force and stiffness results with negligible error,
- Soft magnetic materials are assumed to be perfect (permissibility $= \infty$), have four ring magnets,
- Curl of M is zero everywhere, hence J_v=0, and the Fourier transformation can expand $J_s(x, \mathrm{y})$ to axial direction $J_s(x, \xi)$,
- Relative permeability of axially magnetized PMs is one (μ_r=1) and the equivalent surface current density of radially magnetized PMs for stator and rotor are noted by $J_{s(\mathrm{radial})}(x, \xi)$ and $J_{r(\mathrm{radial})}(x, \xi)$ respectively.

Figures 2(a) and 2(b) depict that it is possible to arrange the ring PMs on the both sides of iron yoke having optimum air gap length, as well as using iron cores in between and at the back of ring PM, as depicted in the corresponding Figures 2(c) and 2(d). In constructing PMBs, it is assumed that the magnet's width and the iron's width are alike. In Figure 2, letters represent the respective dimensions such as PM height, width, air gap length, height of iron yoke and design is done based on Table 1. Likewise, h stands for the length of the air gap. By taking the y-coordinate, situated at midpoint of the gap length, the equation is expressed by (1).

$$x_i = h/2\,, then\ \ x_{ij} = x_i + w_p \tag{1}$$

The ratio of the stiffness to unit length (K_x,K_y) of the proposed 2D model, radial and axial rigidity (K_{axial}, $\mathrm{K}_{\mathrm{radial}}$) are calculated using (2). The optimized design parameters presented in Table 1 were obtained from [69], [70].

$$K_{axial} = 2\pi * r_n * K_y \ and\ K_{radial} = 2\pi * r_n * K_x \tag{2}$$

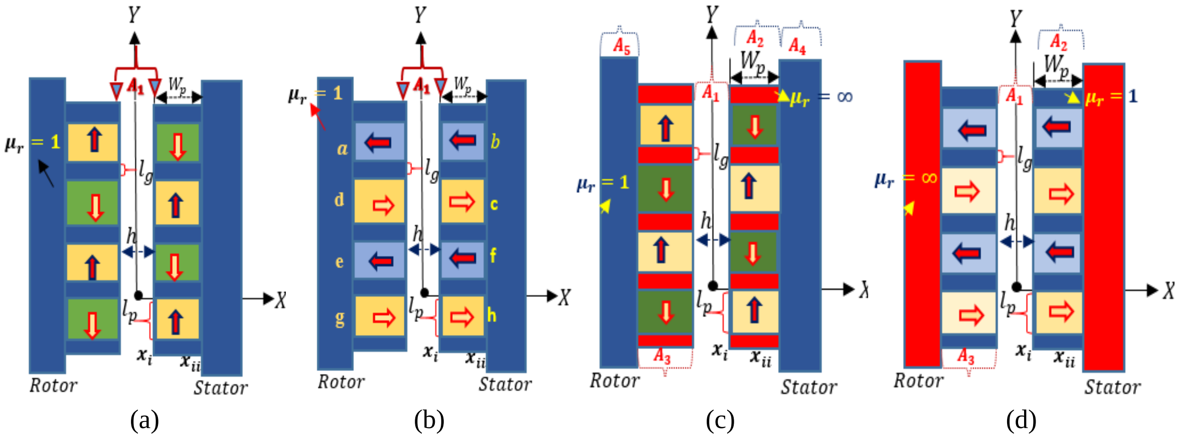

Figure 2. Topologies of PMB studied: (a) standard rotating, (b) without air gap, (c) iron core between the rings, and (d) iron core at the back of ring magnets

Table 1. Optimized design parameters

Constraints	Unit	Material used
Air gap length (l_g)	0.2 mm	Neodymium (rotors ring)
Ring magnet height (l_p)	$1\ mm \le l_p \le 10\ mm$	
Ring magnet width (w_p)	$1\ mm \le w_p \le 13\ mm$	
Radius of PMB (r)	$20\ mm \le w_r \le 30\ mm$	Ferrite magnet (stator ring)
Magnetic force (F)	$190\ N \le F \le 220\ N$	
Remanent flux density (B_r)	1.15 T	

3. DESIGN ANALYSIS

Magnetic field distribution analysis is done using the 2D FE method, and simulation is done based on the above assumptions. In the 2D model, the space is discretized in to small elements, and for each element, the result of the Fourier transformation analysis is done by the separation variable technique Figure 3 [71]–[74].

3.1. Standard and rotating configuration of PMBs

Poisson's equation can be used to calculate a rotating array's magnetic vector potential. There are two currents for a rotating array positioned between $x{=}x_i$ and $x{=}x_{ii}$ sources resulting from axially magnetized PMs $J_{\text{axial}}(\xi)$ in planes of $x{=}x_i$ and $x{=}x_{ii}$ and a current source $J_{\text{radial}}(\xi)$ in $x_i{<}x{<}x_{ii}$ so that poison's equation can be written for the PMs that are radially magnetized as (3).

$$\nabla^2 A = -\mu_0 J_{axial}(\xi)\delta(x - x_i) + \mu_0 J_{axial}(\xi)\delta(x - x_{ii}) + \mu_0 J_{radial}(\xi)u(x - x_{ii}) - \mu_0 J_{radial}(\xi)u(x - x_i) \quad (3)$$

By utilizing the variable separation method and by applying superposition law and the sum of the magnetic vector potentials for the rotor and stator can be used to get the overall solution as shown on (4).

$$A = \mu_o \int_{-\infty}^{\infty} \left(\frac{J_{ax}}{|\xi|} + \frac{J_{ra}}{\xi^2}\right)\left(\frac{e^{-|\xi|xi} - e^{-|\xi|xii}}{2}\right)\left(e^{|\xi|x} + \eta e^{-|\xi|x - j\xi y_e}\right)e^{j\xi y}\, d\xi, for\ the\ x = x_i \quad (4)$$

3.2. Standard radial configuration with back iron

Radially oriented bearings feature two ring structures nested inside one another with an air-gap as shown in Figure 2. Much effort has been done to numerically estimate the force and stiffness of these structures under axial and radial magnetization schemes. In the study of radial PMBs, the element is discretized into three areas A_1, A_2, and A_3. The vector potential analyzed in these three areas is given by (5)-(7) [75].

$$A_1 = \int_{-\infty}^{\infty}\left[F_2(\xi)e^{\xi x} + G_2(\xi)e^{-\xi x}\right] e^{j\xi x d\xi}, for|x| \le x_i \quad (5)$$

$$A_2 = \int_{-\infty}^{\infty}\left[F_3(\xi)\cosh(\xi(x - x_{ii})) + \frac{J_{radial}}{\xi^2}\right] e^{j\xi y}\, d\xi, for x_i < x < x_{ii} \quad (6)$$

$$A_3 = \int_{-\infty}^{\infty} \left[F_1(\xi)\cosh(\xi(x + x_{ii})) + \frac{\eta J_{radial} e^{-\xi ye}}{\xi^2} \right] e^{j\xi y} d\xi, for - x_{i_i} < x < -x_i \quad (7)$$

3.3. Axial magnetic bearing having iron core in between ring magnets

While considering the iron core in the middle of ring magnets can cause the Laplace equation in non-periodic space to have a very complicated integral form. Thus, the (y) axis magnetic field distribution can be determined by Fourier analysis as depicted on (8) and (9) [76].

$$A_q = \sum(a_{qn}e^{k_n x} + b_{qn}e^{-k_n x})e^{ik_n y}\; but, K_n = \frac{n\pi}{L}, n = \pm1, \pm3, \pm5 \quad (8)$$

$$L = L_g + L_b \quad (9)$$

Value of (q) can be inserted to the regions(A_1), (A_4), and (A_5) by using this equation and L_b taken as overall length of PMB to get solution of infinite areas. The Maxwell stress tensor is used to determine the electromagnetic force on the rotor. The summation performed on infinite range of domain with $(x=0)$ and for a length z-axies. The overall summation may be assessed by Fourier on in the given domain area using Parseval's theorem as (10) [77]:

$$F_x = \frac{1}{2\mu_o}\int_{-\infty}^{\infty}({B_x}^2 - {B_y}^2)d\xi\; ; and F_y = \frac{1}{\mu_o}\int_{-\infty}^{\infty} B_x B_y d\xi \quad (10)$$

The resulting ‘magnetic fields’ obtained through examining solutions of vector potential. Forces are calculated by substituting magnetic fields on (11) and obtained (12).

$$F_x = \frac{1}{2\mu_o}\int_0^1({B_x}^2 - {B_y}^2)dy\; ; and F_y = \frac{1}{\mu_o}\int_0^1(B_x B_y)dy \quad (11)$$

$$F_x = \sum\frac{2l}{\mu_o}[a_{1n}{b_{1n}}^* + b_{1n}{a_{1n}}^*]{k_n}^2, and, F_y = \sum\frac{2l}{\mu_o}[a_{1n}{b_{1n}}^* - b_{1n}{a_{1n}}^*]{k_n}^2, (for, n = 1{,}3) \quad (12)$$

Stiffness of both axial and radial magnetization is determined by deriving equation with respect to the corresponding y_e and h, respectively (13).

$$k_y = -\frac{\partial F_y}{\partial y_e} and k_x = -\frac{\partial F_x}{\partial h}; k_x or k_y = \sum\frac{-2{k_n}^2}{l\mu_o}\left[a_{1n}\frac{\partial b_{1n}}{\partial h} + {b_{1n}}^*\frac{\partial a_{1n}}{\partial h} \pm b_{1n}\frac{\partial {a_{1n}}^*}{\partial h} \pm {a_{1n}}^*\frac{\partial b_{1n}}{\partial h}\right] for(n = 1{,}3\ldots\infty) \quad (13)$$

4. RESULTS AND DISCUSSION

The FE method accurately studies radial and axial magnetization, considering geometry-related topology, non-linearity, and high-quality mesh, as shown in Figures 3(a) and 3(b). Accurate characterization of PMB properties is crucial for its use in mechanical systems, involving altering radial and axial positions to observe forces and stiffness obtained by the interaction of magnetic flux. For the standard type of PMBs with axial and radial configurations as depicted on Figures 4(a) and 4(b), there is a 1.29% deviation in magnetic flux density, an almost similar magnetic flux density distribution, which can be used as a reference to discuss the remaining three cases.

Figures 5(a) and 5(b) depict the magnetic flux density on axial and radial-configured PMBs with an air gap in between ring magnets. Hence, the insertion of an air gap in between the rings will increase magnetic flux density by 94.64% in axial and 25.54% in radial configurations as compared with the standard above. Similar study reported on 2 and 3 ring PMBs, but a slight deviation is due to the additional number of ring magnets used here.

Figures 6(a) and 6(b) show that the insertion of an iron core at the back will increase magnetic flux density by 40.52% in axial and 20.20% in radial configurations with respect to the standard. For axially configured PMBs having an iron core in between the ring magnets, the magnetic flux density is decreased by 1.32% and increased for radially configured PMBs by 24.14%, as depicted in Figures 7(a) and 7(b). The magnetic flux density distribution on four ring magnets for a given configuration have good agreement with the findings on 2 and 3 ring magnet PMBs.

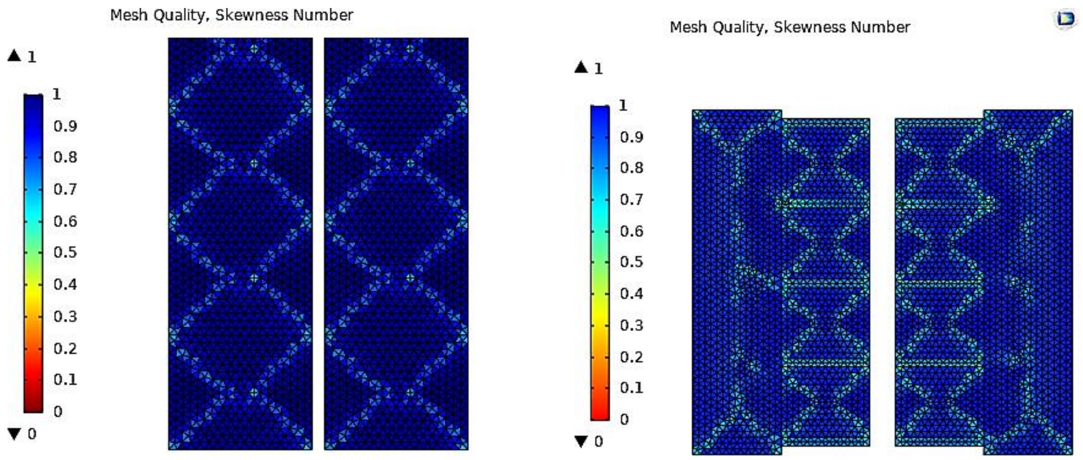

(a) (b)

Figure 3. Mesh quality considered for the study, quality skewness ranges (0.7-0.95), (a) ring with air gap and (b) ring with back iron

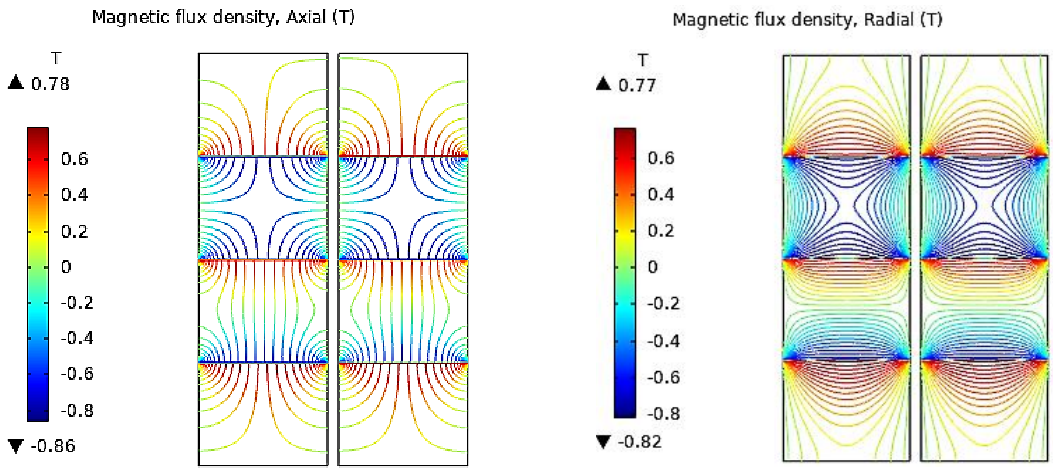

(a) (b)

Figure 4. Standard magnetic flux distribution for (a) axial PMB and (b) radial type PMB

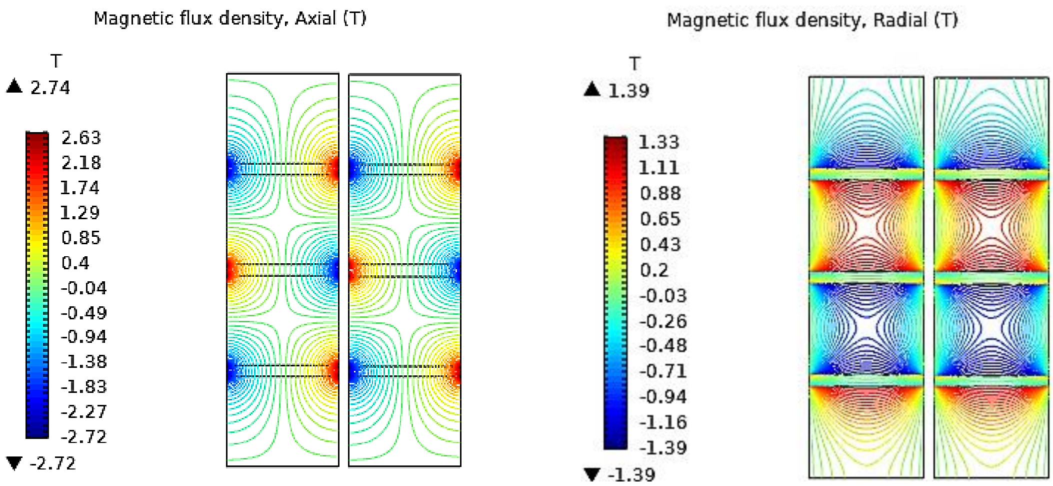

(a) (b)

Figure 5. Magnetic flux distribution ring magnets with air gap in between them for (a) axial and (b) radial type PMB

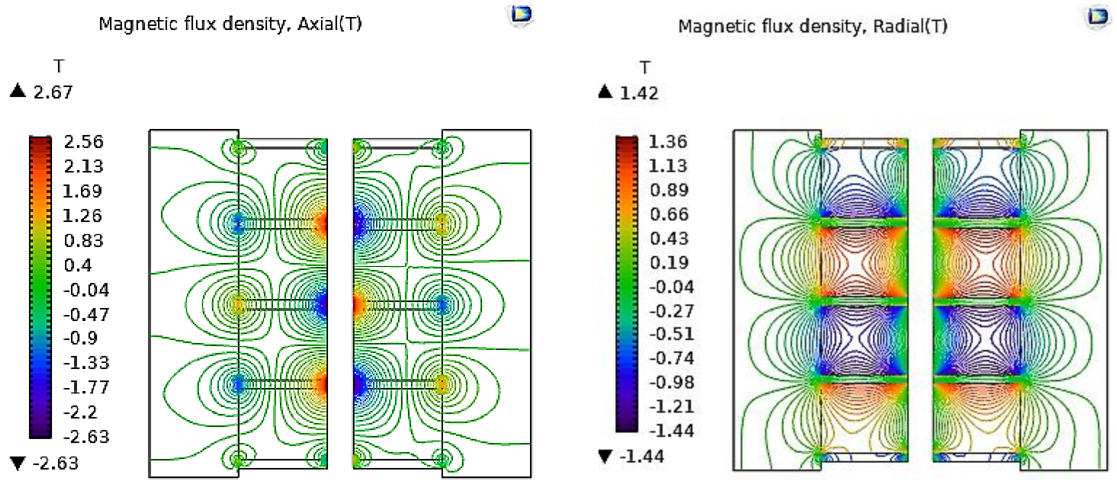

(a) (b)

Figure 6. Magnetic flux distribution on ring magnets with iron core at the back of them for (a) axial and (b) radial type PMB

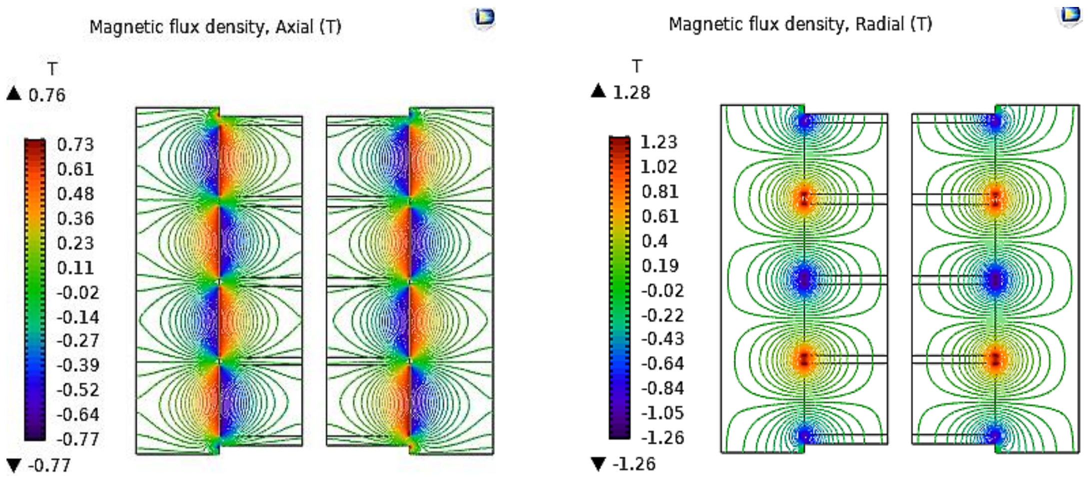

(a) (b)

Figure 7. Magnetic flux distribution ring magnets with iron core in between them, for (a) axial and (b) radial type PMB

There are eight (4-pair) pieces of ring magnets used for such 2D analysis; see Figure 2(b). Figures 8-10 depict each segment having a different color and showing the corresponding magnet ring, while doing simulation (a), (b), (c), (d), (e), (f), (g), and (h) depicts the individual segments of ring magnets in Figure 2(b), and then the line graph shows trends of magnetic flux density versus phase angle for both axially and radially configured ring magnets in the rotor and stator ring of bearing in the four scenarios.

Figures 8–10 depict the trend of magnetic flux density (ϕ) distribution versus phase angle for both axial and radial configurations of PMBs. It comes from the fact that when the ring magnet is perpendicular to the field, small repulsive movements of it led to changes in the flux. As shown in Figures 8(a), 9(a), and 10(a), eight different curves of (ϕ) each have a maximum, which means they counter-intuitively have a big flux change in smaller change in phase.

But, radial configuration, Figures 8(b), 9(b), and 10(b) show that the ring is "flat" in that the condition of attraction or repulsion does not change the flux a lot. According to the relation between magnetic flux and electromotive force (emf), some of the ring magnets have a zero magnetic flux line, which indicates the maximum emf . The graph depicts the phase or time derivative of magnetic flux, based on the properties of sine and cosine. The cosine represents maximum flux, while zero means no flux. Figure 11, displays a concise overview of the distribution of magnetic flux density in both the axial and radial orientations for four distinct configurations of PMBs, labeled as A, B, C, and D. As mentioned earlier, the magnetic flux density (Mnfn) exhibits an increase in all four cases (A-D) for PMBs configured in a radial manner.

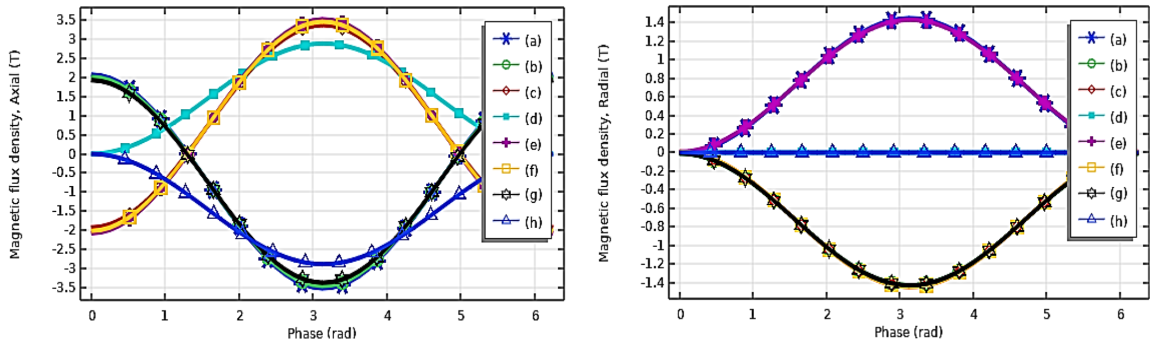

(a) (b)

Figure 8. Standard magnetic flux distribution on eight ring magnets for (a) axial PMB and (b) radial type PMB

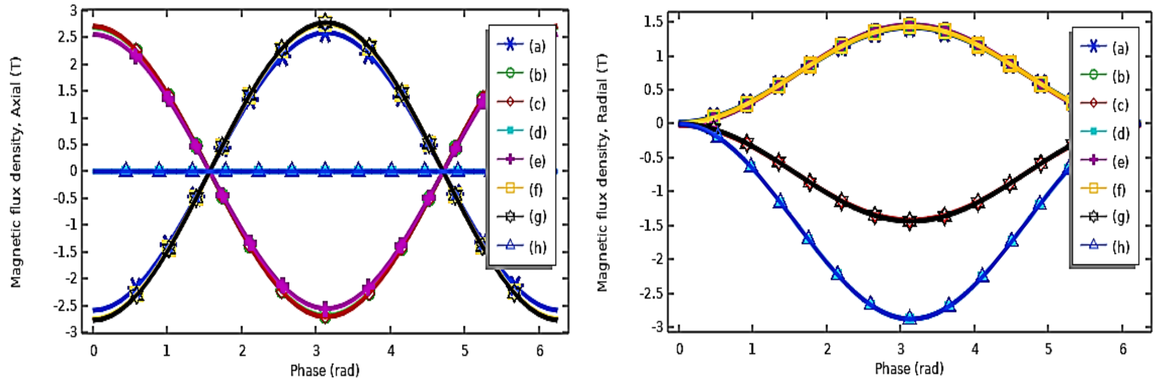

(a) (b)

Figure 9. Magnetic flux distribution on eight ring magnets with air gap in between them for (a) axial and (b) radial type PMB

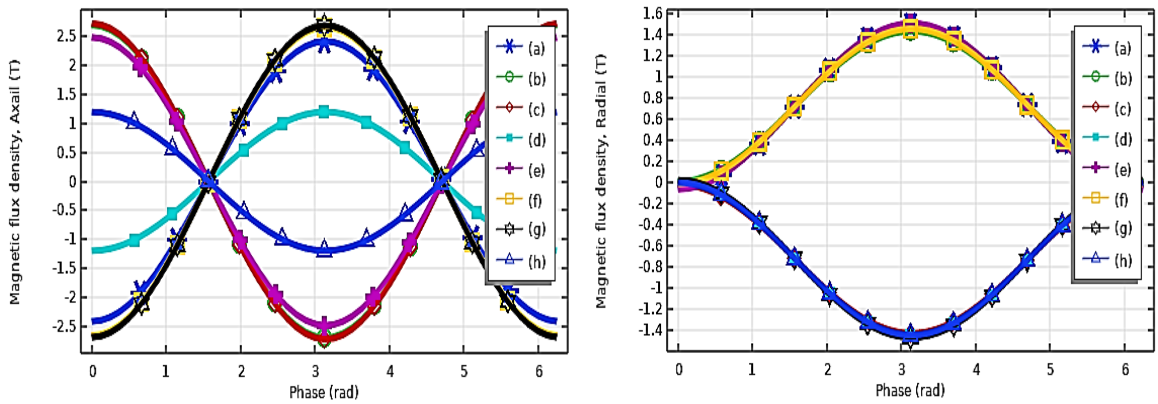

(a) (b)

Figure 10. Magnetic flux distribution on eight ring magnets with iron core at the back of them for (a) axial and (b) radial type PMB

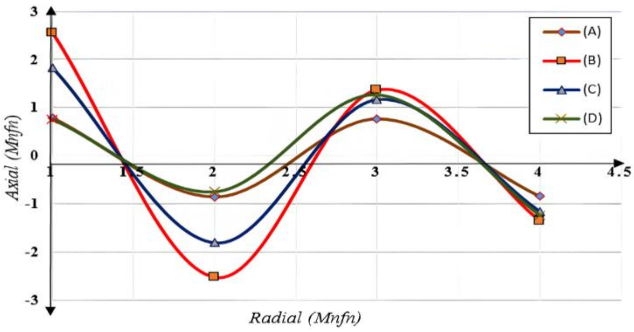

Figure 11. Four configurations of PMBs: (a) standard, (b) air gap in between ring, (c) iron core at back, and (d) iron core between rings

5. CONCLUSION

The interaction between the inner and outer ring magnets generates repulsive forces that efficiently reduce the friction between the rotating parts. The configurations, having air gaps and soft magnetic materials, including iron core in between ring magnets and iron core at the back, will increase magnetic flux density, which is a key factor in increasing the stiffness of the PMBs. By incorporating iron cores into the rear portion and strategically placing air gaps between the ring magnets, the rigidity of the structure has been significantly enhanced. Furthermore, the PMB offers the distinct advantage of not requiring any control system or external power source. Consequently, a conventional arrangement that involves stacking radially magnetized PMs, along with back iron and optimal air gaps between the ring magnets, is extremely well-suited for integration into a compact and small-scale wind turbine.

REFERENCES

[1] P. Karimi, A. K. Darban, and Z. Mansourpour, "A finite element model to simulate magnetic field distribution and laboratory studies in wet low-intensity magnetic separator," *Journal of Mining and Environment*, vol. 10, no. 3, pp. 717–727, 2019, doi: 10.22044/jme.2019.8132.1680.

[2] J. Sun, D. Chen, and Y. Ren, "Stiffness Measurement Method of Repulsive Passive Magnetic Bearing in SGMSCMG," *IEEE Transactions on Instrumentation and Measurement*, vol. 62, no. 11, pp. 2960–2965, Nov. 2013, doi: 10.1109/TIM.2013.2256818.

[3] Z. Yu, G. Zhang, Q. Qiu, L. Hu, D. Zhang, and M. Qiu, "Analysis of Levitation Characteristics of a Radial-Type High-Temperature Superconducting Bearing Based on Numerical Simulation," *IEEE Transactions on Applied Superconductivity*, vol. 25, no. 3, pp. 1–5, Jun. 2015, doi: 10.1109/TASC.2014.2368453.

[4] E. Marth, G. Jungmayr, and W. Amrhein, "A 2-D-Based Analytical Method for Calculating Permanent Magnetic Ring Bearings With Arbitrary Magnetization and Its Application to Optimal Bearing Design," *IEEE Transactions on Magnetics*, vol. 50, no. 5, pp. 1–8, May 2014, doi: 10.1109/TMAG.2013.2295550.

[5] J. G. Storey, M. Szmigiel, F. Robinson, S. C. Wimbush, and R. A. Badcock, "Stiffness Enhancement of a Superconducting Magnetic Bearing Using Shaped YBCO Bulks," *IEEE Transactions on Applied Superconductivity*, vol. 30, no. 4, pp. 1–6, Jun. 2020, doi: 10.1109/TASC.2020.2982884.

[6] S. I. Babic and C. Akyel, "Improvement in the analytical calculation of the magnetic field produced by permanent magnet rings," *Progress In Electromagnetics Research C*, vol. 5, pp. 71–82, 2008.

[7] I. Masaie, K. Demachi, T. Ichihara, and M. Uesaka, "Numerical Evaluation of Rotational Speed Degradation in the Superconducting Magnetic Bearing for Various Superconducting Bulk Shapes," *IEEE Transactions on Appiled Superconductivity*, vol. 15, no. 2, pp. 2257–2260, Jun. 2005, doi: 10.1109/TASC.2005.849625.

[8] L. Ai, G. Zhang, W. Li, G. Liu, J. Chen, and Q. Qiu, "Simplified calculation for the radial levitation force of radial-type superconducting magnetic bearing," *IET Electric Power Applications*, vol. 12, no. 9, pp. 1291–1296, Nov. 2018, doi: 10.1049/iet-epa.2018.0063.

[9] L. Zhang, H. Wu, P. Li, Y. Hu, and C. Song, "Design, Analysis, and Experiment of Multiring Permanent Magnet Bearings by Means of Equally Distributed Sequences Based Monte Carlo Method," *Mathematical Problems in Engineering*, vol. 2019, pp. 1–17, Jul. 2019, doi: 10.1155/2019/4265698.

[10] A. Cansiz, I. Yildizer, E. A. Oral, and Y. Kaya, "An Effective Noncontact Torque Mechanism and Design Considerations for an Evershed-Type Superconducting Magnetic Bearing System," *IEEE Transactions on Applied Superconductivity*, vol. 24, no. 1, pp. 22–29, Feb. 2014, doi: 10.1109/TASC.2013.2280033.

[11] X. Sun, B. Su, L. Chen, Z. Yang, and K. Li, "Design and analysis of interior composite-rotor bearingless permanent magnet synchronous motors with two layer permanent magnets," *Bulletin of the Polish Academy of Sciences Technical Sciences*, vol. 65, no. 6, pp. 833–843, Dec. 2017, doi: 10.1515/bpasts-2017-0091.

[12] B.-U. Koehler, J. Denk, G. Van Maanen, and M. Lang, "Applying Standard Industrial Components for Active Magnetic Bearings," *Actuators*, vol. 6, no. 1, p. 8, Feb. 2017, doi: 10.3390/act6010008.

[13] Y. Yuan, Y. Sun, and Q. Xiang, "Design and Analysis of a Magnetic Bearings with Three Degrees of Freedom," *Chinese Journal of Mechanical Engineering*, vol. 32, no. 1, p. 3, Dec. 2019, doi: 10.1186/s10033-019-0320-3.

[14] P. T. Micha, T. Mohan, and S. Sivamani, "Design and Analysis of a Permanent Magnetic Bearing for Vertical Axis Small Wind Turbine," *Energy Procedia*, vol. 117, pp. 291–298, Jun. 2017, doi: 10.1016/j.egypro.2017.05.134.

[15] A. Filatov, L. Hawkins, and P. McMullen, "Homopolar Permanent-Magnet-Biased Actuators and Their Application in Rotational Active Magnetic Bearing Systems," *Actuators*, vol. 5, no. 4, p. 26, Dec. 2016, doi: 10.3390/act5040026.

[16] R. Safaeian and H. Heydari, "Comprehensive comparison of different structures of passive permanent magnet bearings," *IET Electric Power Applications*, vol. 12, no. 2, pp. 179–187, Feb. 2018, doi: 10.1049/iet-epa.2017.0308.

[17] Y. Zhao, X. Chen, F. Wang, C. Wei, and Y. Zhao, "Modeling of active magnetic bearing in rotating payload satellite considering shaft motion coupling," *Journal of Mechanical Science and Technology*, vol. 34, no. 11, pp. 4423–4437, Nov. 2020, doi: 10.1007/s12206-020-1005-7.

[18] K. Falkowski, P. Kurnyta-Mazurek, T. Szolc, and M. Henzel, "Radial Magnetic Bearings for Rotor–Shaft Support in Electric Jet Engine," *Energies*, vol. 15, no. 9, p. 3339, May 2022, doi: 10.3390/en15093339.

[19] R. Ravaud, G. Lemarquand, and V. Lemarquand, "Force and Stiffness of Passive Magnetic Bearings Using Permanent Magnets. Part 2: Radial Magnetization," *IEEE Transactions on Magnetics*, vol. 45, no. 9, pp. 3334–3342, Sep. 2009, doi: 10.1109/TMAG.2009.2025315.

[20] A. Hamler, V. Goričan, B. Štumberger, M. Jesenik, and M. Trlep, "Passive magnetic bearing," *Journal of Magnetism and Magnetic Materials*, vol. 272–276, pp. 2379–2380, May 2004, doi: 10.1016/j.jmmm.2003.12.972.

[21] J.-P. Yonnet, G. Lemarquand, S. Hemmerlin, and E. Olivier-Rulliere, "Stacked structures of passive magnetic bearings," *Journal of Applied Physics*, vol. 70, no. 10, pp. 6633–6635, Nov. 1991, doi: 10.1063/1.349857.

[22] P. Samanta and H. Hirani, "Magnetic Bearing Configurations: Theoretical and Experimental Studies," *IEEE Transactions on Magnetics*, vol. 44, no. 2, pp. 292–300, Feb. 2008, doi: 10.1109/TMAG.2007.912854.

[23] S. I. Bekinal and S. Jana, "Generalized Three-Dimensional Mathematical Models for Force and Stiffness in Axially, Radially, and Perpendicularly Magnetized Passive Magnetic Bearings With 'n' Number of Ring Pairs," *Journal of Tribology*, vol. 138, no. 3, Jul. 2016, doi: 10.1115/1.4032668.

[24] R. Ravaud, G. Lemarquand, and V. Lemarquand, "Force and Stiffness of Passive Magnetic Bearings Using Permanent Magnets. Part 1: Axial Magnetization," *IEEE Transactions on Magnetics*, vol. 45, no. 7, pp. 2996–3002, Jul. 2009, doi: 10.1109/TMAG.2009.2016088.

[25] D. Meeker, "Finite Element Method Magnetics : Magnetics Tutorial," *WikkaWiki*, 2013.

[26] A. Filatov and L. Hawkins, "Comparative study of axial/radial magnetic bearing arrangements for turbocompressor applications," *Proceedings of the Institution of Mechanical Engineers. Part I: Journal of Systems and Control Engineering*, vol. 230, no. 4, pp. 300–310, 2016, doi: 10.1177/0959651815593649.

[27] B. Aeschlimann, M. Hubatka, R. Stettler, and R. Housseini, "Commissioning of Off-Shore Gas Compressor With 9-Axes Magnetic Bearing System: Commissioning Tools," in *Volume 9: Oil and Gas Applications; Supercritical CO2 Power Cycles; Wind Energy*, Jun. 2017. doi: 10.1115/GT2017-64182.

[28] L. J. Wu, Z. Q. Zhu, D. Staton, M. Popescu, and D. Hawkins, "An Improved Subdomain Model for Predicting Magnetic Field of Surface-Mounted Permanent Magnet Machines Accounting for Tooth-Tips," *IEEE Transactions on Magnetics*, vol. 47, no. 6, pp. 1693–1704, Jun. 2011, doi: 10.1109/TMAG.2011.2116031.

[29] T. Lubin, S. Mezani, and A. Rezzoug, "Development of a 2-D Analytical Model for the Electromagnetic Computation of Axial-Field Magnetic Gears," *IEEE Transactions on Magnetics*, vol. 49, no. 11, pp. 5507–5521, Nov. 2013, doi: 10.1109/TMAG.2013.2267746.

[30] M. Cheng, P. Han, G. Buja, and M. G. Jovanovic, "Emerging Multiport Electrical Machines and Systems: Past Developments, Current Challenges, and Future Prospects," *IEEE Transactions on Industrial Electronics*, vol. 65, no. 7, pp. 5422–5435, Jul. 2018, doi: 10.1109/TIE.2017.2777388.

[31] M. Cheng, H. Wen, P. Han, and X. Zhu, "Analysis of Airgap Field Modulation Principle of Simple Salient Poles," *IEEE Transactions on Industrial Electronics*, vol. 66, no. 4, pp. 2628–2638, Apr. 2019, doi: 10.1109/TIE.2018.2842741.

[32] J. M. Crider and S. D. Sudhoff, "An Inner Rotor Flux-Modulated Permanent Magnet Synchronous Machine for Low-Speed High-Torque Applications," *IEEE Transactions on Energy Conversion*, vol. 30, no. 3, pp. 1247–1254, Sep. 2015, doi: 10.1109/TEC.2015.2412547.

[33] Y. Gao, D. Li, R. Qu, and J. Li, "Design Procedure of Flux Reversal Permanent Magnet Machines," *IEEE Transactions on Industry Applications*, vol. 53, no. 5, pp. 4232–4241, Sep. 2017, doi: 10.1109/TIA.2017.2695980.

[34] P. Krause, O. Wasynczuk, S. D. Sudhoff, and S. Pekarek, "Theory of Electromechanical Energy Conversion," in *Analysis of Electric Machinery and Drive Systems*, Wiley, 2013, pp. 1–52. doi: 10.1002/9781118524336.ch1.

[35] H. Y. Li and Z. Q. Zhu, "Influence of magnet arrangement on performance of flux reversal permanent magnet machine," in *2017 IEEE International Electric Machines and Drives Conference (IEMDC)*, May 2017, pp. 1–8. doi: 10.1109/IEMDC.2017.8002029.

[36] H.-Y. Li, Y. Liu, and Z. Q. Zhu, "Comparative Study of Air-Gap Field Modulation in Flux Reversal and Vernier Permanent Magnet Machines," *IEEE Transactions on Magnetics*, vol. 54, no. 11, pp. 1–6, Nov. 2018, doi: 10.1109/TMAG.2018.2837898.

[37] I. Petrov, M. Niemela, P. Ponomarev, and J. Pyrhonen, "Rotor Surface Ferrite Permanent Magnets in Electrical Machines: Advantages and Limitations," *IEEE Transactions on Industrial Electronics*, vol. 64, no. 7, pp. 5314–5322, Jul. 2017, doi: 10.1109/TIE.2017.2677320.

[38] Y. Shi, L. Jian, J. Wei, Z. Shao, W. Li, and C. C. Chan, "A New Perspective on the Operating Principle of Flux-Switching Permanent-Magnet Machines," *IEEE Transactions on Industrial Electronics*, vol. 63, no. 3, pp. 1425–1437, Mar. 2016, doi: 10.1109/TIE.2015.2492940.

[39] L. Wu, R. Qu, D. Li, and Y. Gao, "Influence of Pole Ratio and Winding Pole Numbers on Performance and Optimal Design Parameters of Surface Permanent-Magnet Vernier Machines," *IEEE Transactions on Industry Applications*, vol. 51, no. 5, pp. 3707–3715, Sep. 2015, doi: 10.1109/TIA.2015.2426148.

[40] W. Zhao, J. Zheng, J. Wang, G. Liu, J. Zhao, and Z. Fang, "Design and Analysis of a Linear Permanent- Magnet Vernier Machine With Improved Force Density," *IEEE Transactions on Industrial Electronics*, vol. 63, no. 4, pp. 2072–2082, Apr. 2016, doi: 10.1109/TIE.2015.2499165.

[41] Z. Q. Zhu, H. Y. Li, R. Deodhar, A. Pride, and T. Sasaki, "Recent developments and comparative study of magnetically geared machines," *CES Transactions on Electrical Machines and Systems*, vol. 2, no. 1, pp. 13–22, Mar. 2018, doi: 10.23919/TEMS.2018.8326448.

[42] R. Ravaud, G. Lemarquand, V. Lemarquand, and C. Depollier, "The three exact components of the magnetic field created by a radially magnetized tile permanent magnet," *Progress In Electromagnetics Research*, vol. 88, pp. 307–319, 2008, doi: 10.2528/PIER08112708.

[43] R. Ravaud, G. Lemarquand, and V. Lemarquand, "Halbach structures for permanent magnets bearings," *Progress In Electromagnetics Research M*, vol. 14, pp. 263–277, 2010, doi: 10.2528/PIERM10100401.

[44] M. Van Beneden, V. Kluyskens, and B. Dehez, "Optimal Sizing and Comparison of Permanent Magnet Thrust Bearings," *IEEE Transactions on Magnetics*, vol. 53, no. 2, pp. 1–10, Feb. 2017, doi: 10.1109/TMAG.2016.2625275.

[45] M. Van Beneden, V. Kluyskens, and B. Dehez, "Comparison between optimized topologies of permanent magnet thrust bearings with back-iron," *Mechanical Engineering Journal*, vol. 4, no. 5, pp. 17-00061-17–00061, 2017, doi: 10.1299/mej.17-00061.

[46] E. Marth, G. Jungmayr, M. Panholzer, and W. Amrhein, "Optimization of Stiffness per Magnet Volume Ratio of Discrete and Continuous Halbach Type Permanent Magnetic Bearings," in *13th International Symposium on Magnetic Bearings*, 2012, vol. 180, pp. 1–14.

[47] G. Jungmayr, E. Marth, W. Amrhein, H.-J. Berroth, and F. Jeske, "Analytical Stiffness Calculation for Permanent Magnetic Bearings With Soft Magnetic Materials," *IEEE Transactions on Magnetics*, vol. 50, no. 8, pp. 1–8, Aug. 2014, doi: 10.1109/TMAG.2014.2310437.

[48] I. da Silva, J. R. Cardoso, and O. Horikawa, "Design Considerations for Achieving High Radial Stiffness in an Attraction-Type Magnetic Bearing With Control in a Single Direction," *IEEE Transactions on Magnetics*, vol. 47, no. 10, pp. 4112–4115, Oct. 2011, doi: 10.1109/TMAG.2011.2144959.

[49] R. Moser, J. Sandtner, and H. Bleuler, "Optimization of repulsive passive magnetic bearings," *IEEE Transactions on Magnetics*, vol. 42, no. 8, pp. 2038–2042, Aug. 2006, doi: 10.1109/TMAG.2005.861160.

[50] S. I. Bekinal, T. R. Anil, and S. Jana, "Analysis of axially magnetized permanent magnet bearing characteristics," *Progress In Electromagnetics Research B*, vol. 44, pp. 327–343, 2012, doi: 10.2528/PIERB12080910.

[51] S. I. Bekinal, T. R. R. Anil, and S. Jana, "Analysis of radial magnetized permanent magnet bearing characteristics," *Progress In Electromagnetics Research B*, vol. 47, pp. 87–105, 2013, doi: 10.2528/PIERB12102005.

[52] G. B. Gallego, L. Rossini, T. Achtnich, C. Zwyssig, D. M. Araujo, and Y. Perriard, "Force and Torque Model of Ironless Passive Magnetic Bearing Structures," in *2019 IEEE International Electric Machines & Drives Conference (IEMDC)*, May 2019, pp. 507–514. doi: 10.1109/IEMDC.2019.8785411.

[53] K. P. Lijesh, M. Doddamani, and S. I. Bekinal, "A Pragmatic Optimization of Axial Stack-Radial Passive Magnetic Bearings," *Journal of Tribology*, vol. 140, no. 2, Mar. 2018, doi: 10.1115/1.4037847.

[54] N. Tanase, A. M. Morega, I. Chirita, and C. Ilie, "Passive Magnetic Bearing – Design and Numerical Simulation," in *2019 11th International Symposium on Advanced Topics in Electrical Engineering (ATEE)*, Mar. 2019, pp. 1–5. doi: 10.1109/ATEE.2019.8724949.

[55] P. Bernstein and J. Noudem, "Superconducting magnetic levitation: principle, materials, physics and models," *Superconductor Science and Technology*, vol. 33, no. 3, p. 033001, Mar. 2020, doi: 10.1088/1361-6668/ab63bd.

[56] A. Bossavit, "Numerical modelling of superconductors in three dimensions: a model and a finite element method," *IEEE Transactions on Magnetics*, vol. 30, no. 5, pp. 3363–3366, Sep. 1994, doi: 10.1109/20.312659.

[57] C. Navau and A. Sanchez, "Stiffness and energy losses in cylindrically symmetric superconductor levitating systems," *Superconductor Science and Technology*, vol. 15, no. 10, pp. 1445–1453, Oct. 2002, doi: 10.1088/0953-2048/15/10/313.

[58] Z. Kohari, V. Tihanyi, and I. Vajda, "Loss Evaluation and Simulation of Superconducting Magnetic Bearings," *IEEE Transactions on Appiled Superconductivity*, vol. 15, no. 2, pp. 2328–2331, Jun. 2005, doi: 10.1109/TASC.2005.849644.

[59] A. Cansiz and D. T. McGuiness, "Optimization of the Force and Stiffness in a Superconducting Magnetic Bearing Based on Particular Permanent-Magnet Superconductor Configuration," *IEEE Transactions on Applied Superconductivity*, vol. 28, no. 2, pp. 1–8, Mar. 2018, doi: 10.1109/TASC.2017.2781178.

[60] X. Ren, M. Feng, and T. Ren, "Design and Optimization of a Radial High-Temperature Superconducting Magnetic Bearing," *IEEE Transactions on Applied Superconductivity*, vol. 29, no. 2, pp. 1–5, Mar. 2019, doi: 10.1109/TASC.2018.2886812.

[61] F. N. Werfel, U. Floegel-Delor, T. Riedel, R. Rothfeld, D. Wippich, and B. Goebel, "HTS Magnetic Bearings in Prototype Application," *IEEE Transactions on Applied Superconductivity*, vol. 20, no. 3, pp. 874–879, Jun. 2010, doi: 10.1109/TASC.2010.2040261.

[62] J. F. P. Fernandes, A. J. A. Costa, and J. Arnaud, "Optimization of a Horizontal Axis HTS ZFC Levitation Bearing Using Genetic Decision Algorithms Over Finite Element Results," *IEEE Transactions on Applied Superconductivity*, vol. 30, no. 2, pp. 1–8, Mar. 2020, doi: 10.1109/TASC.2020.2964546.

[63] J. Xu, Z. Li, X. Yuan, and C. Zhang, "Hybrid-type superconducting magnetic bearings for rotating machinery," in *High-Temperature Superconductors: Occurrence, Synthesis and Applications*, 2018, pp. 307–327.

[64] T. Minami, S. Sakai, and S. Ohashi, "Improvement of stability against vibration at the mechanical resonance in attractive type HTS-permanent hybrid magnet bearing," in *2016 IEEE Region 10 Conference (TENCON)*, Nov. 2016, pp. 3294–3297. doi: 10.1109/TENCON.2016.7848661.

[65] H. Mitsuda, A. Inoue, B. Nakaya, and M. Komori, "Improvement of Energy Storage Flywheel System With SMB and PMB and Its Performances," *IEEE Transactions on Applied Superconductivity*, vol. 19, no. 3, pp. 2091–2094, Jun. 2009, doi: 10.1109/TASC.2009.2019533.

[66] G. G. Sotelo, R. de Andrade, and A. C. Ferreira, "Magnetic Bearing Sets for a Flywheel System," *IEEE Transactions on Applied Superconductivity*, vol. 17, no. 2, pp. 2150–2153, Jun. 2007, doi: 10.1109/TASC.2007.899268.

[67] K. D. Bachovchin, J. F. Hoburg, and R. F. Post, "Magnetic Fields and Forces in Permanent Magnet Levitated Bearings," *IEEE Transactions on Magnetics*, vol. 48, no. 7, pp. 2112–2120, Jul. 2012, doi: 10.1109/TMAG.2012.2188140.

[68] M. W. Kennedy, S. Akhtar, J. A. Bakken, and R. E. Aune, "Analytical and Experimental Validation of Electromagnetic Simulations Using COMSOL , re Inductance , Induction Heating and Magnetic Fields," in *Proceedings of the 2011 COMSOL Conference in Stuttgart*, 2011, p. 9.

[69] M. Lang, "Optimization of permanent-magnet bearings," in *Proceedings of the 6th International Symposium on Magnetic Suspension Technology*, 2001.

[70] J. Sun, H. Zhou, and Z. Ju, "Dynamic Stiffness Analysis and Measurement of Radial Active Magnetic Bearing in Magnetically Suspended Molecular Pump," *Scientific Reports*, vol. 10, no. 1, p. 1401, Jan. 2020, doi: 10.1038/s41598-020-57523-8.

[71] S. Xu and J. Fang, "A Novel Conical Active Magnetic Bearing With Claw Structure," *IEEE Transactions on Magnetics*, vol. 50, no. 5, pp. 1–8, May 2014, doi: 10.1109/TMAG.2013.2295060.

[72] C. S. Siyambalapitiya, "Model and Validation of Static and Dynamic Behavior of Passive Diamagnetic Levitation for Energy Harvesting," *Engineering, Physics*, no. January, pp. 1–155, 2012.

[73] U. H. Hegazy and Y. A. Amer, "A time-varying stiffness rotor-active magnetic bearings system under parametric excitation," *Proceedings of the Institution of Mechanical Engineers, Part C: Journal of Mechanical Engineering Science*, vol. 222, no. 3, pp. 447–458, Mar. 2008, doi: 10.1243/09544062JMES563.

[74] K. K. Nielsen, C. R. H. Bahl, N. A. Dagnaes, I. F. Santos, and R. Bjork, "A Passive Permanent Magnetic Bearing With Increased Axial Lift Relative to Radial Stiffness," *IEEE Transactions on Magnetics*, vol. 57, no. 3, pp. 1–8, Mar. 2021, doi: 10.1109/TMAG.2020.3042957.

[75] H. Eryong and L. Kun, "Investigation of Axial Carrying Capacity of Radial Hybrid Magnetic Bearing," *IEEE Transactions on Magnetics*, vol. 48, no. 1, pp. 38–46, Jan. 2012, doi: 10.1109/TMAG.2011.2167018.
[76] E. Hou and K. Liu, "Tilting Characteristic of a 2-Axis Radial Hybrid Magnetic Bearing," *IEEE Transactions on Magnetics*, vol. 49, no. 8, pp. 4900–4910, Aug. 2013, doi: 10.1109/TMAG.2013.2244098.
[77] K. Falkowski and Z. Gosiewski, "Analytical Method of the Magnetic Force Estimation in Passive Magnetic Bearings," in *The 8th International conference on motion and vibration - control MOVIC*, 2006, no. Movic, pp. 830–835.

BIOGRAPHIES OF AUTHORS

Yang Chaojun received the M.Sc. and Ph.D. degrees from Jiangsu University, Zhenjiang, China, in 1997 and 2013, respectively. She is a professor and a Ph.D. and supervisor in the School of Mechanical Engineering, Jiangsu University. Her current research interests include the analysis and design of magnetic drive machines, laser processing technology, and mechanical transmission. She can be contacted at email: yangchaojun@ujs.edu.cn, or 1000000696@ujs.edu.cn.

Amberbir Wondimu received his B.Sc. in mechanical engineering from Haramaya University and M.Sc. from Addis Ababa Science and Technology University, Ethiopia. Currently, he is pursuing his Ph.D. study at Jiangsu University School of Mechanical Engineering, Zhenjiang, China. His research interests include the modeling and simulation of magnetic gear, magnetic couplers, and magnetic bearings. His dissertation is on magnetic gear and its applications in wind turbine power transmission systems. He can be contacted at email: ambirewondimu@gmail.com.

Ayodeji Olalekan Salau received his B.Eng. in electrical/computer engineering from the Federal University of Technology, Minna, Nigeria. He received the M.Sc. and Ph.D. degrees from the Obafemi Awolowo University, Ile-Ife, Nigeria. His research interests include research in the fields of computer vision, image processing, signal processing, machine learning, control systems engineering and power systems technology. Dr. Salau serves as a reviewer for several reputable international journals. His research has been published in many reputable international conferences, books, and major international journals. He is a registered engineer with the Council for the Regulation of Engineering in Nigeria (COREN), a member of the International Association of Engineers (IAENG), and a recipient of the Quarterly Franklin Membership with ID number CR32878 given by the editorial board of London Journals Press in 2020 for top quality research output. More recently, Dr. Salau's research paper was awarded the best paper of the year 2019 in Cogent Engineering. In addition, he is the recipient of the International Research Award on New Science Inventions (NESIN) under the category of "best researcher award" given by Science Father with ID number 9249, 2020. Currently, Dr. Salau works at Afe Babalola University in the Department of Electrical/Electronics and Computer Engineering. He can be contacted at email: ayodejisalau98@gmail.com.